INTERNATIONAL JOURNAL OF MARITIME TECHNOLOG

IJMT Vol.5/ Winter 2016 (55-62)

Available online at: http://ijmt.ir/browse.php?a_code=A-10-310-1&sid=1&slc_lang=en

Numerical Investigation on the Effect of Tunnel Height on Drag Reduction in a High Speed Trimaran

Hamid Kazemi Moghadam[1], Rouzbeh Shafaghat[2*]

[1]*MSc, Babol Noshirvani University of Technology, Sea Based Energy Research Group, h.kazemi@stu.nit.ac.ir*

[2]*Assistant Professor, Babol Noshirvani University of Technology, Sea Based Energy Research Group, rshafaghat@nit.ac.ir*

ARTICLE INFO

Article History:
Received: 15 Feb. 2016
Accepted: 15 Mar. 2016

Keywords:
High-speed Planing hull
Tunnel height
Dynamic mesh, Drag Reduction
Trimaran

ABSTRACT

There are different methods to reduce drag in high speed hulls. One of these methods is a change in the shape of the body by adding longitudinal side tunnels. In this paper it has been attempted to determine the influence of the tunnel height on hydrodynamic characteristics of the hull to achieving an optimum shape for the tunnel. To achieve this purpose, numerical simulation of the problem has been done using finite volume method considering moving mesh. For turbulence modeling, k-ε model and to simulate free surface, the Volume of Fluid (VOF) two phase model has been employed. The results show that creating a tunnel in the base mono-hull would lead to reduction of the total drag at high speed as well as decreasing the vessel draft of the hull over the whole range. Furthermore, in the Volumetric Froude number around 4, a reduction in the height of the tunnel could decrease the hull drag. In higher Volumetric Froude numbers, reduction of the tunnel height, to some extent, increases the drag with a slight slope.

1. Introduction

Adding longitudinal tunnels in a high speed mono-hull has been introduced as an appropriate method for reducing drag; however, one cannot be certain that creating tunnel in the hull body could reduce the drag or increase the maneuverability ability. Applying tunnel in a hull is only useful when more knowledge is gained about the effective geometric parameters of the tunnel as well as the interaction between the operational parameters in designing the hull. Different geometric parameters in various parts of the tunnel (like the tunnel blade, the tunnel dimensions and its accessories) could influence the hull performance.

In the area of simulating tunneled high speed hulls, few researches have been carried out. Most studies have been devoted to catamaran hulls. Veijia et al. (2013) has experimentally investigated the geometric parameters effective on the blade runner hull [1]. Employing eight experimental samples in their study, they investigated the effect of weight, center of mass and transversal step role on the performance of trimaran hull. Yousefi et al. (2013) changed the cougar high speed mono-hull into a tunneled one and could achieve a 14% of drag reduction in the maximum speed of the hull [2]. Producing a multi-body shell using a numerical and experimental model, Ghassabzadeh and Ghasemi (2013) investigated the hull behavior in different speeds [3,4]. Shen et al (2013) studied the catamaran performance by means of the moving mesh method and compared the obtained results with those of Savitsky and Mori methods [5]. Alexander Gary et al. (2013) attempted to simulate the trimaran shell using CFD tool and compared the results with the experimental ones [6]. H. Kazemi et al. (2015) investigated the tunnel aperture on drag reduction in a tunneled planing hull numerically [7]. Najafi and et al (2015) investigated influence interceptor effect on hydrodynamic parameters of planing catamarans [8].

In most works presented about the tunneled high speed hulls, the performance has been investigated based on an existing design of a tunneled shell. In this research, performance of the tunneled hull has been initially studied by changing an existing mono-hull shell into a tunneled one (compared to the based mono-hull), and then the influence of the tunnel height on drag reduction has been evaluated in the form of a parametric investigation. In Figure 1, Bladerunner that is a high speed trimaran hull is illustrated.

Various geometric parameters of the side tunnels are effective on performance of the tunneled hulls. These

parameters could be categorized into two main groups of tunnel dimensions and its accessories.

Figure 1. Bladerunner, High speed Trimaran Hull [11]

The tunnel accessories consist of parts like the steps in the tunnel ceiling, longitudinal steps and the tunnel blade. Four parameters of aperture, height, length of the tunnel as well as the blade height are accounted as main dimensional parameters. Among the mentioned parameters, investigating the role of the tunnel height on variations of the hull drag is the purpose of this research. To do so, a high speed mono-hull has been changed into a tunneled hull keeping the main frame and based on the method of converting a mono-hull into a tunneled one introduced by Yousefi et al. (2013); then, different geometries have been independently generated through making changes in the height of the tunnel [2]. The goal of producing shells with different tunnels has been parametric investigation of the influences of tunnel height on performance of the hull in reducing drag.

2. Generating the Geometry

As mentioned above, the tunneled body has been generated through keeping the main frame of a mono-hull (Figure 2) whose purpose has been considered as a planing mono-hull model. In table 1 the geometric parameters of the base hull as well as the base tunneled hull have been presented; according to table 1, the base mono-hull has length of 100 cm, height of 14.4 cm, maximum width of 31 cm and the maximum deadrise angle of 26 degrees. To achieve an overall pattern in order to produce the tunneled body from the geometry of a mono-hull, the tunneled hull is divided into three main parts which, independently, have the largest effect on the hydrodynamic performance of the hull.

1. Prismatic Body, where the most important parameters, including the prismatic width of the body, the floor deadrise angle in each longitudinal cross section and their variations profile along the length are considered.
2. Tunnel, where the most important parameters consist of the tunnel width, the tunnel height and their variation profiles along the hull length as well as the shape of the tunnel cross section.
3. Tunnel Blade, where the main parameters are the deviation angle, height and the variations profile along the hull length.

Due to this categorization, one could easily come to the conclusion that a tunneled hull is formed by combination of two parts: the tunnel and the prismatic body. Accordingly, the floor deflection angle, the prism width, the tunnel cross section, width and height of the tunnel in each section, the transversal variations and the blade height of the hull as well as its gunwale could be determined. The best method of smoothing the built volume from connecting the longitudinal sections would be a consistency in variations of these parameters based on the hull length. In this case, one should specify the function of each parameter along the hull in order for the variations curve of parameters to be continuous and for the generated volume to be totally smooth. To form an effective interrelation between the parameters, specific dimensionless numbers have been used through which one could obtain the geometric characteristics of a tunneled hull by introducing 5 points and having width, height and deadrise angle of each section of the base hull (Figure 2).

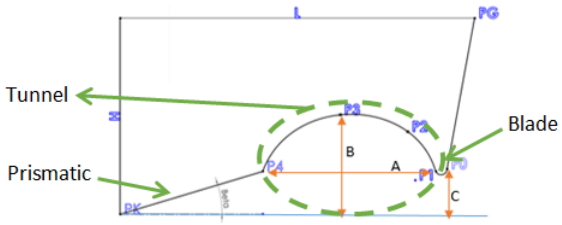

Figure 2. Different parameters of the tunneled hull section

After determining the geometric characteristics of the necessary transversal sections along the length of the hull, the geometric parameters of the tunneled hull could be completely specified and the initial form of the tunneled hull model would be obtained (Figure 3).

Table 1. Geometric characteristics of the base mono-hull and the initial tunneled hull

Geometric Characteristics	Unit	Tunneled	Mono-hull
Hull Length	cm	100	100
Beam	cm	31	31
Overall Height	cm	14.4	14.4
Mean Deadrise	deg	26	26
Hull Weight	kg	3.19	3.19
Volume Displacement	kg	24.47	20.9
Center Of Mass	cm	20	20
Initial Trim	deg	4	6.5
Initial Drift	cm	6.93	8.7
Number of Tunnels		-----	2
Tunnel Height	cm	-----	7.1
Tunnel Aperture	cm	-----	7.8

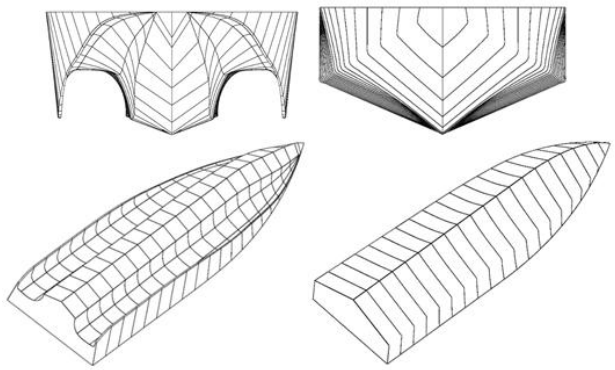

Figure 3. The base mono-hull and the tunneled hull generated in different views

Now in order to investigate and improve the hydrodynamic performance of the tunneled hull, different geometries are produced by changing the tunnel height parameter. In order to study the effects of the height variations, the dimensions have been increased or decreased by 10 percent of the initial values. This increase or decrease in the height proceeds until more variations show no considerable enhancement in the hull drag. In figure 4, picture d shows the initial hull (base) with height of 7.8 cm. An increase of 10 percent in the tunnel height, shell e could be obtained. The shells could be observed based on the height reduction of the hull in three images of a, b and c getting smaller by 10, 20 and 30 percent of the initial tunnel height, respectively.

Table 2. Characteristics of the investigated tests

Test Name	Shell Name	Ratio of the Tunnel Height to the Hull Height	Tunnel Height	Ratio of the Hull Aperture to the Width	Tunnel Aperture
Case 1	a	0.4	57	0.5	78
Case 2	b	0.45	64	0.5	78
Case 3	c	0.5	71	0.5	78
Case 4	d	0.55	78	0.5	78

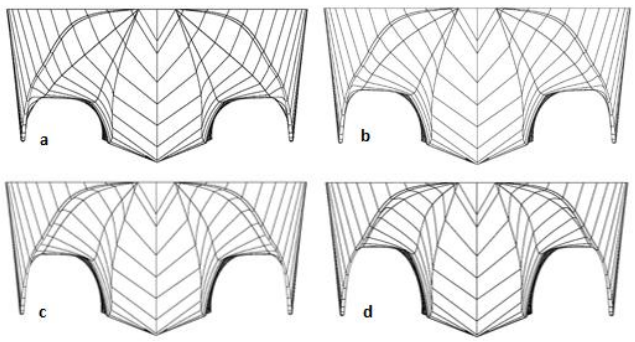

Figure 4. Hulls profiles (a) 20 percent decrease in the tunnel height (b) 10 percent decrease in the tunnel height (c) the initial tunneled hull (base) (d) 10 percent increase in the tunnel height

3. Governing Equations

Assuming the flow as incompressible, mass conservation equation (continuity) is as followed:

$$div\ U = 0 \tag{1}$$

where U is the velocity vector.

To express the momentum conservation equation, Navier-Stokes equations have been employed:

$$\begin{aligned}
&\frac{\partial(\rho u)}{\partial t} + div(\rho u U) = -\frac{\partial P}{\partial x} + div(\mu.grad(u)) \\
&\frac{\partial(\rho v)}{\partial t} + div(\rho v U) = -\frac{\partial P}{\partial y} + div(\mu.grad(v)) \\
&\frac{\partial(\rho w)}{\partial t} + div(\rho w U) = -\frac{\partial P}{\partial z} + div(\mu.grad(w)) - \rho g
\end{aligned} \tag{2}$$

where P is the static pressure exerted on the fluid, μ is the fluid viscosity and u, v and 2 are the components of the velocity vector.

In case that the flow has free surface and according to changes in the shapes of the free surface, and the waves-breaking phenomenon, modeling the free surface, is of considerable importance. In another work Yousefi et al. (2013), using a benchmarking procedure, studied the methods of solving the flow over the high speed hulls; according to this benchmarking approach, the most appropriate method for simulating the free surface and VOF approach is based on the free surface capturing method [9]. In this case a transport equation is solved for calculating the fluid two phase volume of Fluid. The transport equation of the volume Fluid (equation (3)) is obtained based upon the continuity equation which is calculated according to incompressibility of two phases and after solving transfer, density and fluid viscosity from equation (4).

$$\frac{\partial \alpha}{\partial t} + \nabla.(\alpha u) = 0 \tag{3}$$

$$\begin{aligned}
&\rho_{eff} = \alpha.\rho_1 + (1-\alpha).\rho_2 \\
&\nu_{eff} = \alpha.\nu_1 + (1-\alpha).\nu_2
\end{aligned} \tag{4}$$

Where α is a number between zero and one and, in fact, it reflects the percentage of presence of each fluid in the computational domain.

Turbulence has been modeled by means of k-ε two-equation model. In k-ε model, the turbulent field is expressed in terms of two variables- Turbulent Kinetic Energy, k, and the rate of viscosity dissipation of the turbulent kinetic energy, ε, which are obtained through transport differential equations 5 and 6.

$$\frac{\partial(\rho k)}{\partial t} + \nabla\cdot(\rho U k) = \nabla\cdot\left(\left(\mu + \frac{\mu_t}{\sigma_k}\right)\nabla k\right) + P_k - \rho\varepsilon \tag{5}$$

$$\frac{\partial(\rho \varepsilon)}{\partial t} + \nabla\cdot(\rho U \varepsilon) = \nabla\cdot\left(\left(\mu + \frac{\mu_t}{\sigma_\varepsilon}\right)\nabla \varepsilon\right) + \frac{\varepsilon}{k}\left(C_{\varepsilon 1}(P_k) - C_{\varepsilon 2}\rho\varepsilon\right) \tag{6}$$

4. Numerical Solution

4.1 Meshing the Solution Domain and Defining the Boundary Conditions

The Gambit software was then used to generate a three-dimensional mesh. According to the importance of analyzing the flow behavior around and over the hull, meshes of size 3 to 10 mm have been used and four boundary layers mesh with 0.05 cm first layer size employed (Figure 5). For instance, the mesh on the tunneled body has been displayed in figure 5; as is obvious here in the figure, the smallest mesh size has been formed on the tunnel blade. Around the body, the unstructured meshing with tetrahedral elements has been used due to complexity of the geometry.

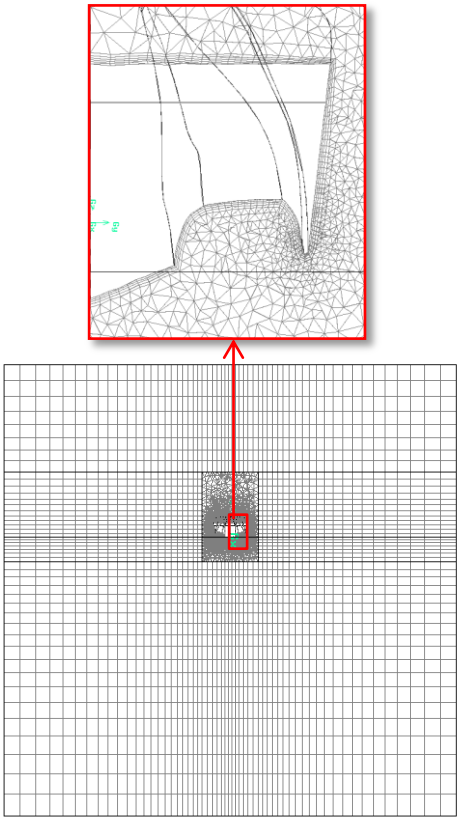

Figure 5. The boundary layer mesh on the tunneled hull body

To reduce the number of cells in the zones far from the body, the structured mesh with cubic hexahedral elements have been employed. In order to achieve this purpose solution domain divided to seven sections (Figure 6). The computational domain dimensions have been shown in this figure. For the free surface, the mesh of size 1 to 2 cm and in the regions far from the body a meshing of size 4 to 8 cm with an increasing trend has been used. In numerical simulation of the fluid flow, one should identify the type and physics of the flow in the domain boundaries in addition to the mathematic issues of solving the equations. The boundary condition for the inlet (water and air area) has been velocity inlet which is used to define the flow velocity and all scalar properties of the flow at the inlet. The outlet boundary condition for determining the fluid pressure at the outlet is the pressure outlet condition. For the solution domain in the side walls, the symmetric boundary condition has been selected due to its better convergence.

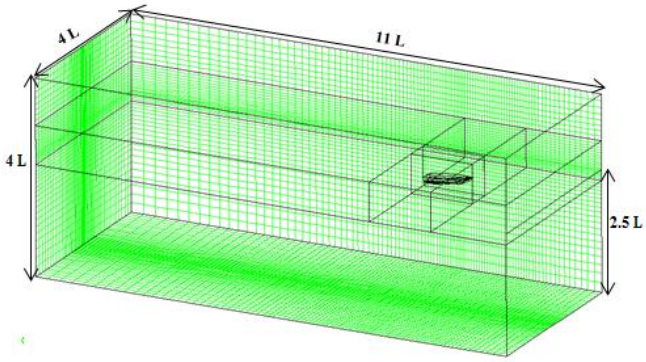

Figure 6. The computational domain dimensions and blocking

The last and the most important boundary condition is moving boundary on which the boundary displacement should be applied. The wall boundary condition is chosen no-slip condition, so that the real model of the hull body could be obtained by inducing shear stress on it. The computational domain and boundary condition have been shown in figure 7.

4.2 Problem solution parameters

In this problem, transient analysis have been used to obtain different values in various times. The time step is obtained based on Courant number of 0.3 for different velocities. For the surface tension coefficient, an amount of 0.073 N/m has been applied. Other settings have been shown in table3.

Table 3. The settings used in the ANSYS-FLUENT software and the numerical solution method

Title	Solution Method	
Solver	Unsteady, Segregated, implicit, dynamesh	
Multi-phase Method	VOF	
Discretization method	Volume Fraction	Compressive
	Momentum	Second Order Upwind
	Pressure	Presto
	Turbulent kinetic energy (k)	Second order upwind
	Viscous dissipation rate (ε)	First order upwind

5. Results and Discussions

In this section the results related to the validation and mesh independency have been initially presented and, then, the results achieved from forming the tunnel in the base hull body have been investigated.

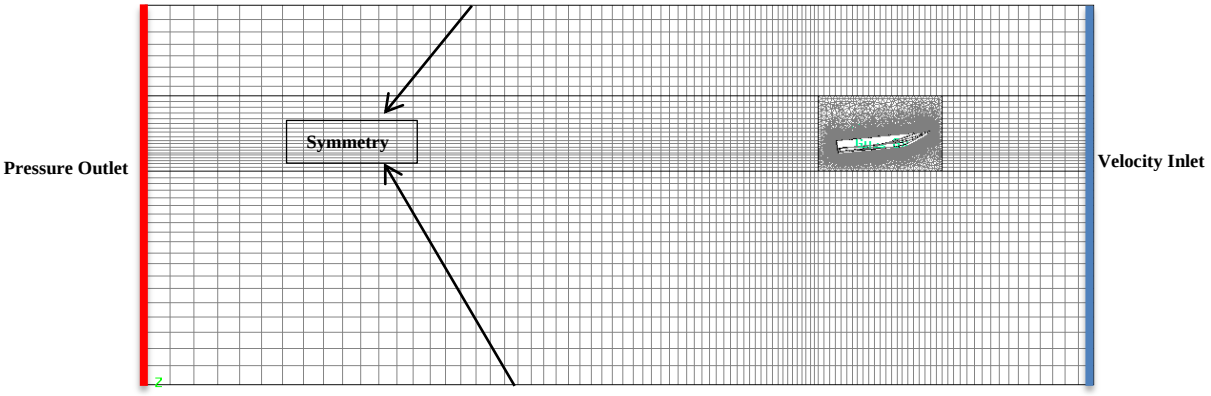

Figure 7. The computational domain and boundary condition

In the final part, the results related to the effect of the tunnel height on the hull performance have been presented.

5.1 Validation and Studying the Mesh Independency of the Solution

In order to validate the numerical solution, the semi empirical method of Savitsky (1964) has been employed [10]. Savitsky is a valid method for predicting the resistance and hydrodynamic parameters of the high speed planing hull. Making drag dimensionless in terms of the hull weight, the mesh independency of the solution for the initial tunneled hull and in the velocity of 10 m/s has been demonstrated in figure 8a. The values obtained for different Volumetric Froude numbers for two methods of numerical and Savitsky have been displayed in figure 8b as well.

5.2 - Investigating the Effect of adding Tunnel in the Hull

According to figure 9a, total drag of the hull has been increased by increase the speed; however, making the tunnel in the hull body has led to the lower total drag of the hull compared to the initial one in high speeds and after reaching the planing mode. This is despite the fact that in low speeds and before the planing mode, the total drag of the tunneled hull is more than that of the initial one.

For better study of the hull behavior, two hydrodynamic parameters of trim angle and the hull immersion depth are considered which have been made dimensionless for better comparison by initial trim and the initial draft, respectively. Based on figure 9b, the mono-hull trim has a uniform and decreasing trend by an increase in the velocity; however, different behavior has been observed about the tunneled hull: before approaching the planing mode, the hull trim is increased and after this mode, the trim exhibits a decreasing trend.

About the hull draft and according to figure 9c, similar behavior has been observed for both mono-hull and multi hull shells; the way that in both shells increasing the velocity leads to a uniform decrease in the hull draft. Furthermore, the ratio of draft over the initial draft is smaller in the tunneled hull compared to the mono-hull.

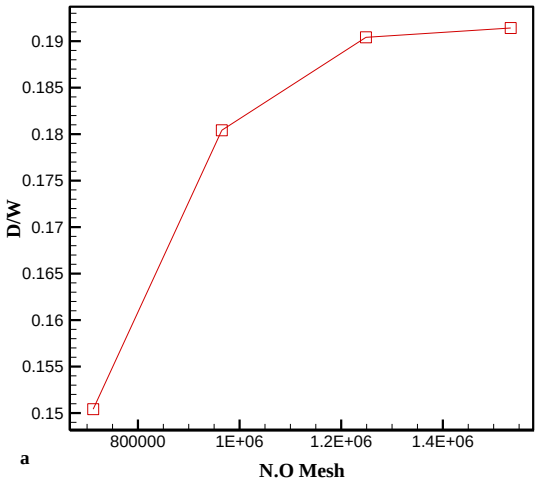

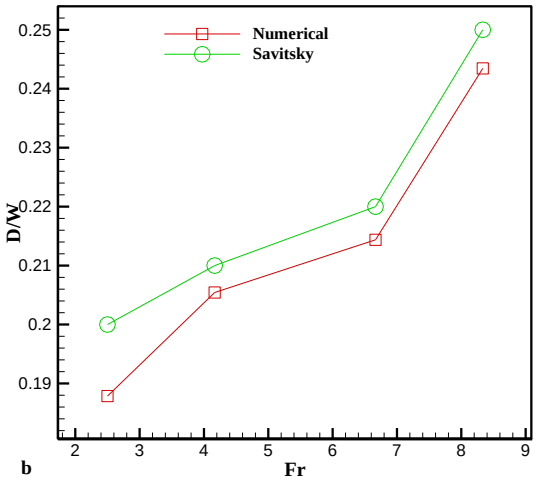

Figure 8. (a) Investigation of the mesh independency (b) Validating the solution

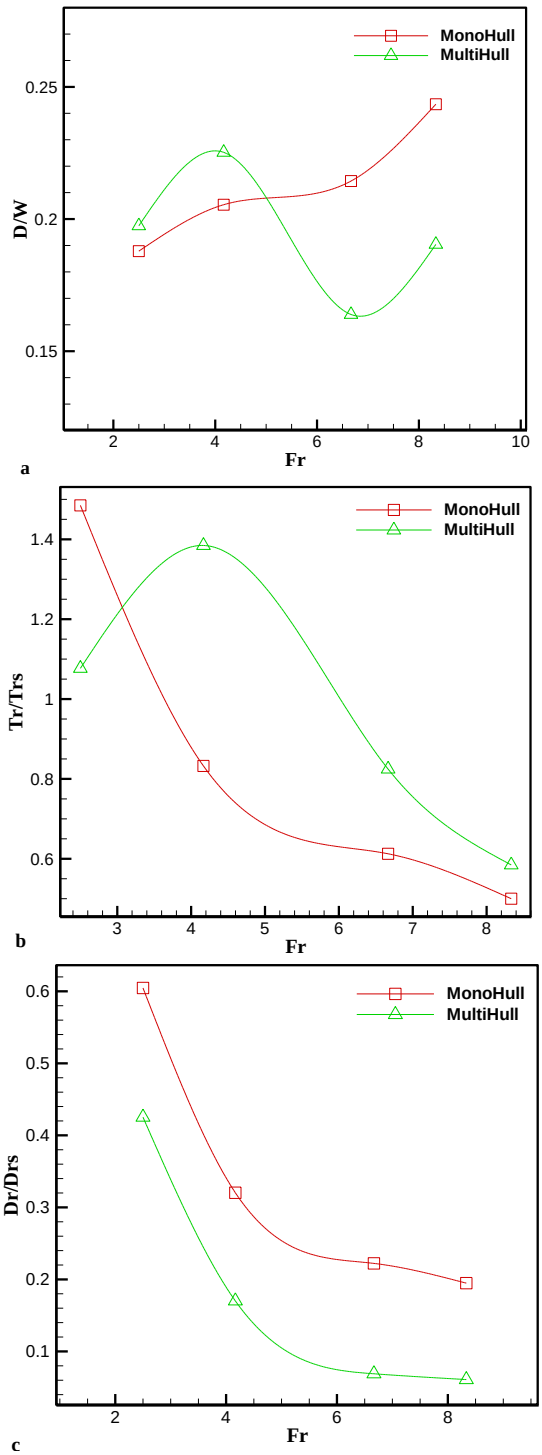

Figure 9. The changes in hydrodynamic parameters by forming a tunnel in the base hull (a) drag diagram (b) trim diagram and (c) draft diagram

5.3 Investigating the Effect of the Tunnel Height on the Hull Performance

Figure 10 shows the wave pattern at velocity rang 3m/s to 10 m/s. Due to figure 11a, one could state that the tunnel height parameter is more effective in transition from low speed mode to planing mode and in the displacement mode it is less effective. A remarkable decline could be observed in the drag through decreasing the tunnel height in the transition region from low speed mode to planing mode.

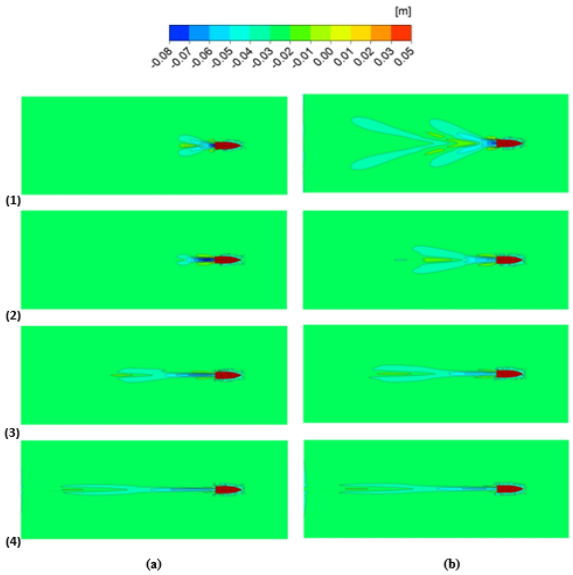

Figure 10. The wave pattern in (a) the tunneled hull and (b) the base mono-hull and in different velocities (1) 3m/s, (2) 5 m/s, (3) 8 m/s, (4) 10 m/s

In figure 11b, the trim variations have been shown in terms of the Volumetric Froude number in the studied cases. According to the obtained results, the tunnel height is effective in the transition region only and this influence does not follow a similar trend. The hull trim is reduced initially by increasing the tunnel height and then an increasing trend takes place.

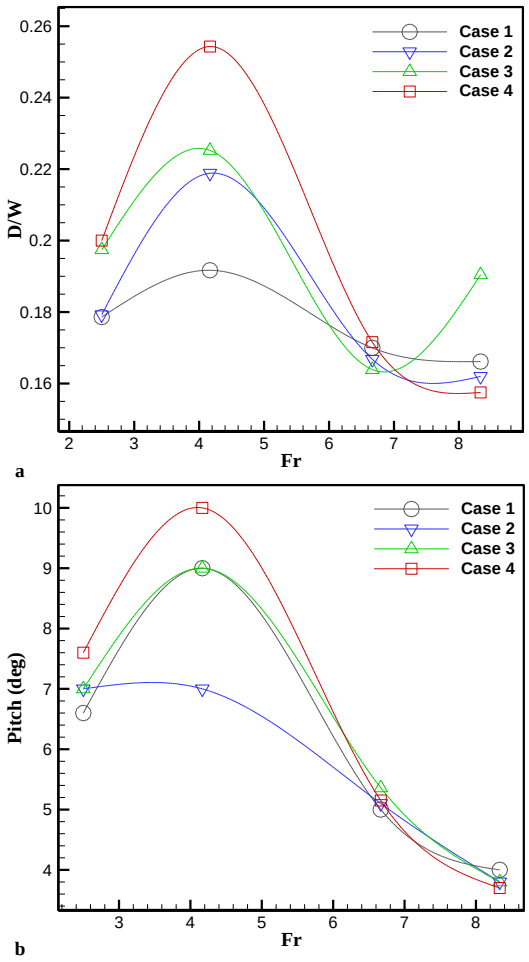

Figure 11. Effect of height (a) drag changes (b) trim angle changes

Figure 12 shows the volume of fluid contour at velocity of 5 m/s. Due to this figure, Reducing the tunnel height, leads to contacting the water with the rear section of tunnel and the tunneled hull with smaller height has had greater contact surface. It is worth noting that due to the impact of water, pressure of the end section of the tunnel has been increased and the trim angle will be reduced.

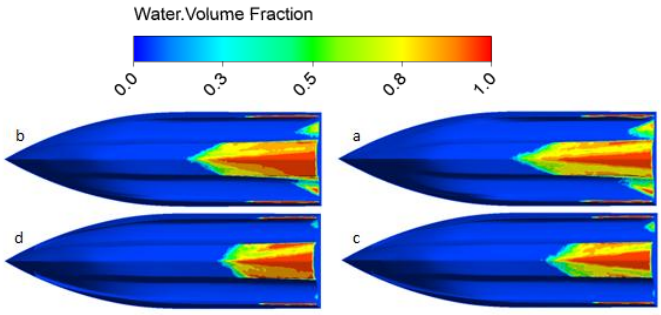

Figure 12. The volume of fluid at the velocity of 5 m/s (a) Case 1, (b) Case 2, (c) Case 3, (d) Case 4

In figure 13, static pressure diagram on the tunnel ceiling has been demonstrated. To draw this graph, one should define a longitudinal line on the ceiling between inlet (0.8) and outlet (-0.2) of the tunnel. As is obvious from figure 13, for a large part of the tunnel, the applied pressure remains unchanged and the pressure changes will occur in a small part (less than 0.1 m) of the end of the tunnel.

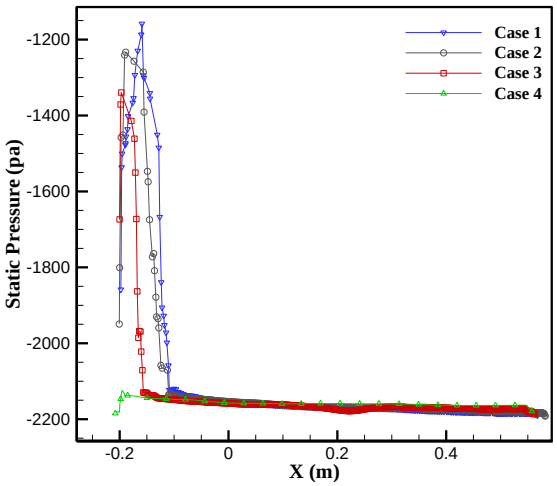

Figure 13. The static pressure on the tunnel ceiling

Figure 14 shows trim angle of four cases at velocity of 5 m/s. As mentioned before, trim and the projected frontal area the flow has been reduced, reducing the height of the tunnel that cause pressure drag reduction; but due to figure 11a, one could not reduce the tunnel height to a specific limit, because it could cause drag increase at high speeds.

Figure 14. Trim of tunneled hull at 5 m/s (a) Case 1, (b) Case 2, (c) Case 3, (d) Case 4

6. Conclusions

As observed in this survey, the shape of a high speed hull has been initially changed into a tunneled form by maintaining main geometric parameters of the hull, such as deadrise angle, keel line, hull width and hull length. In order to achieve an optimum shape for the tunnel, the effect of the tunnel height on hydrodynamic characteristics of the hull has been investigated. Simulation has been performed by dynamic mesh.

Converting a mono-hull into a tunneled one at the beginning of the study, one could observe a draft reduction and trim increase in the planing mode of the hull and, thereafter, a drag improvement after the volumetric Froude number of 5. Drag reduction in the planing mode has been also increased by more than 20%. Through reducing the tunnel height, trim and the projected frontal area the flow has been reduced, that cause pressure drag reduction. In addition high pressure zone and the maximum pressure have been increased as well and led to the drag reduction due to a decline in the draft amount and exiting more parts of the shell from the water surface that cause viscous drag reduction.

List of Symbols

A	Width of the tunnel
B	Height of the tunnel
C	Blade Height
Fr	Volumetric Froude
D	Drag
Dr	Draft
Tr	Trim angle
W	Weight

8. References

1. Weijia Ma, Huawei Sun, Jin Zou, Heng Yang: *Test research on the resistance performance of high-speed*

trimaran Planing hull, Polish maritime Research, No 4/2013.

2. Yousefi R, Shafaghat R, Shakeri R: *High-speed Planing hull drag reduction using tunnels*, Ocean Engineering 84 (2014) 54–60.

3. Ghassabzadeh M, Ghassemi H: *Determining of the hydrodynamic forces on the multi-hull tunnel vessel in steady motion*. J Braz. Soc. Mech. Sci. Eng. DOI 10.1007/s40430-013-0110-2,2014.

4. Ghassabzadeh M, Ghassemi H: *Numerical Hydrodynamic of Multihull Tunnel Vessel. Open Journal of Fluid Dynamics*, 2013, 3, 198-204,2014.

5. Hailong SHEN, Wei Lu and Yumin SU: *Numerical Prediction Method of Resistance Performance of Catamaran Planing Vessels*, Applied Mechanics and Materials Vol. 344 pp 19-22,2013.

6. K Muljowidodo and et al. *Design and simulation analysis of flying trimaran USV. Indian Jurnal of Geo-marian science*. Indian Jurnal of Geo-marine Sciences, Vol. 41 (6), pp. 569-574,2013.

7. Hamid Kazemi Moghadam, Rouzbeh Shafaghat, Reza Yousefi, *Numerical investigation of the tunnel aperture on drag reduction in a high-speed tunneled planing hull*, J Braz. Soc. Mech. Sci. Eng , Volume 37, Issue 6, pp 1719-1730, 2015.

8. A. Najafi, S. Alimirzazadeh, M. Seif, *RANS simulation of interceptor effect on hydrodynamic coefficients of longitudinal equations of motion of planing catamarans*, J Braz. Soc. Mech. Sci. Eng. 37:1257–1275, 2015.

9. Yousefi R, Shafaghat R, Shakeri M: *Hydrodynamic analysis techniques for high-speed Planing hulls*, Applied Ocean Research 42 105–113,2013.

10. Savitsky, D: *Hydrodynamic analysis of Planing hulls*. Mar. Technol. 1 (1), 71–95,1964.

11. Website: http://www.icemarine.com/models/